Numerical Study of the Wingtip Fence on the Wing Airfoil E562 with Fence Height Variations

S. P. Setyo Hariyadi, Sutardi, Wawan Aries Widodo, and Bambang Juni Pitoyo

Abstract Winglets are equipment that must be used by aircraft and unmanned aerial vehicles (UAV) in the modern era. The function of the winglet is to block the fluid flow jump from the lower side to the upper side on an aircraft wing. With the reduction of fluid flow jumps, it is expected that the wing's aerodynamic performance will increase. The researchers mostly made geometric variations of the winglets to obtain maximum results, namely the increase of lift and decreasing drag. This research was conducted using Ansys Fluent 19.0 with a turbulent model k-ω SST. The freestream flow rate to be used is 10 m/s ($Re = 2.34 \times 10^4$) with the angle of attack (α) = 0°, 2°, 4°, 6°, 8°, 10°,12°, 15°, 16°, 17°, 19° and 20°. The model of the specimen is an Eppler 562 airfoil with forward and rearward wingtip fence. From this study, it was found that a winglet with fence height equals the chord line length resulting in better aerodynamic performance than winglet with fence height equal to half the chord line length. It this shows that the winglet with fence height equals the chord line length which can reduce the fluid flow jump from the lower side to the upper side. It was also found that the use of the wingtip fence reduced the strength of vorticity magnitude on the z-axis compared to plain wings. This is due to the vorticity effect of the plain wing and wingtip fence on the flow of fluid passing through it.

Keywords Winglet · Wingtip fence · Lift · Drag · E562

1 Introduction

The world of aviation requires continuous innovation. The intended innovation is not only in the use of fuel but also in aspects related to fuel savings. These fuel savings are closely related to the aerodynamic performance of the aircraft. Geometry modification is the thing most often used by researchers to improve the aerodynamic

S. P. Setyo Hariyadi (✉) · B. J. Pitoyo
Aviation Polytechnic of Surabaya, Surabaya, Indonesia
e-mail: hudzaifahsetyo@gmail.com

Sutardi · W. A. Widodo
Mechanical Engineering Department, Industrial Technology Faculty, Sepuluh Nopember Institute of Technology, Surabaya, Indonesia

U. Sabino et al. (eds.), *Proceedings of the 6th International Conference and Exhibition on Sustainable Energy and Advanced Materials*, Lecture Notes in Mechanical Engineering,
https://doi.org/10.1007/978-981-15-4481-1_36

performance of an object. This geometry modification has the main goal of increasing lift force as high as possible and reducing drag as low as possible.

Geometry modifications in aircraft are mostly carried out on wings. Airplane wings are one of the most important parts of designing an airplane. This is because the aircraft's wings play an important role in producing lift force on the aircraft. The main force components in an aircraft consist of weight, lift force, thrust, and drag. Lifting force works against the direction of the load so that the aircraft can fly.

Sohn and Chang [8] conducted experimental research to see the effect of adding Whitcomb's winglet to vortex wingtip on NACA 631-212 airfoil. The results obtained are wingtip vortices on the wings with Whitcomb's winglet having a weaker and more spreading configuration than simple wing fairing. This causes an increase in the Whitcomb's winglet C_L/C_D.

Yen and Fei [10] also conducted an experimental study to see the effect of the addition of dihedral winglet to vortex wingtip on NACA 0012 airfoil with variations in cant angle $\delta = -30°$, $\delta = 15°$, $\delta = 30°$, $\delta = 45°$, $\delta = 90°$, $\delta = 135°$. The results obtained are at $\delta = 90°$ the value of the lift-to-drag ratio under stall conditions and the maximum value of the lift-to-drag ratio is 32 and 17% greater than without winglet.

The research of Myilsamy et al. [5] produced a comparison chart of C_L, C_D and C_L/C_D for each type of winglet against the angle of attack. In this study, it was shown that the C_L ratio for each type of winglet against the angle of attack, the C_L graph tends to rise to the angle of attack 14°. In the C_D comparison for each type of winglet against the angle of attack, it tends to rise to the angle of attack 14°. In the ratio of lift to drag ratio for each type of wing-let to the angle of attack, C_L/C_D tends to rise to the angle of attack 8° and then decreases to the angle of attack 14°.

In this simulation study comparing the height of the wingtip fence so that it can be seen its effect on aerodynamic performance and other properties behind the UAV wing.

2 Research Methodology

2.1 Computational Fluids Dynamic

This research was carried out using Ansys 19.0 with turbulent k-ω SST models. The flow velocity used is 10 m/s ($Re = 2.34 \times 10^4$) with the angle of attack (α) = 0°, 2°, 4°, 6°, 8°, 10°,12°, 15°, 16°, 17°, 19° and 20°. The test specimen is in the form of plain wing airfoil E562 with variations in winglet geometry. The winglet used is the wingtip fence in the form of forward and rearward. Reynolds Number is determined by chord length. In this case, the length of the chord used is 20 cm. Figure 1 is a simulation domain and boundary conditions used in the simulation Mulvany et al. [4]. The specimen model is a plain wing airfoil type Eppler 562 with a winglet attached to the tip of a wingtip fence as shown in Fig. 2.

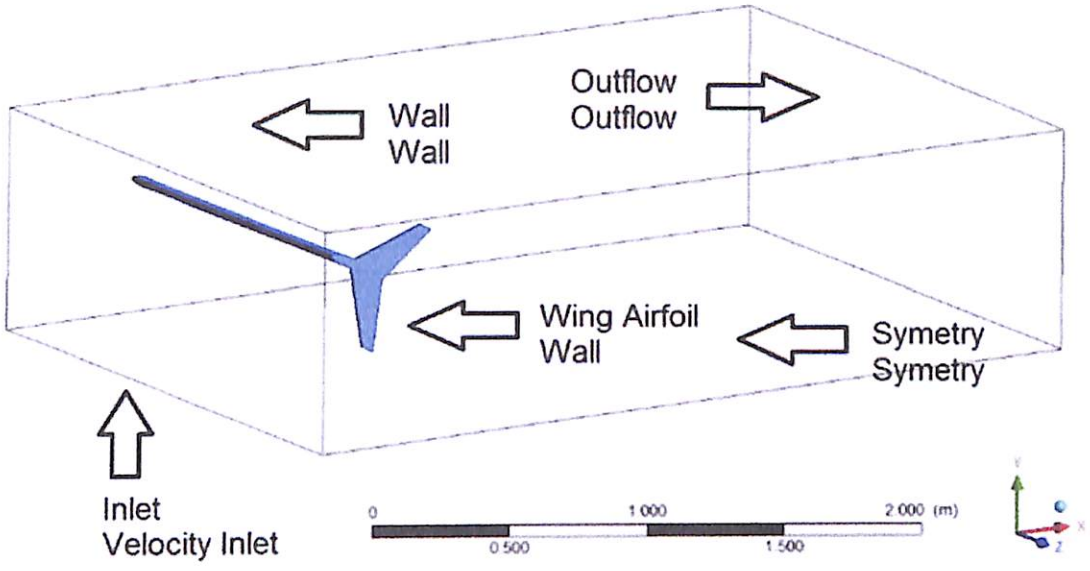

Fig. 1 Simulation domain and boundary conditions

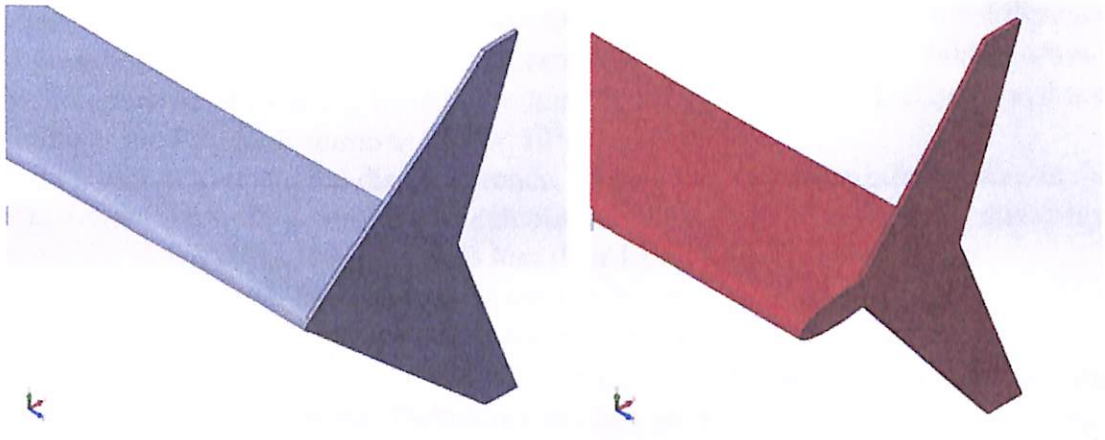

(a) Forward Wingtip Fence (b) Rearward Wingtip Fence

Fig. 2 Specimens model

In numerical simulations, geometry, meshing, and boundary types are made for the test objects. The next step is to do the meshing process and determine the boundary type of the specimens.

The conditions of the environment are entered at a temperature of 30 °C and a pressure of 1 atm. The working fluid conditions included include viscosity (μ) = 1.86×10^{-5} Ns/m^2, (ρ) = 1.17 kg/m^3, length scale at the inlet side of 0.024 m, and turbulence intensity in numerical modeling this is 0.8%.

Table 1 Grid of independence from research [7]

Meshing type	Cells number	Inflation layer	C_D	y^+	Skewness average
Meshing A	875962	40	0.91	1.4	0.348
Meshing B	768003	40	0.90	0.8	0.351
Meshing C	685063	40	0.92	2.1	0.334
Meshing D	569233	40	0.90	0.8	0.343
Meshing E	469620	40	0.88	1.4	0.347
Meshing F	367075	40	0.86	2.1	0.346

2.2 Grid Independence

Grid independence is done to get the amount of meshing that tends to be constant so that the modeling results are close. In this independence grid, the amount of meshing is divided into several types of meshing. The grid independence criteria use the resulting C_D results. The numerical C_D difference is chosen based on the smallest difference value. The most optimal results will be obtained if the difference in drag coefficient with the previous meshing is approximately 2%. Table 1 shows the comparison of meshing from the independence grid with the 3-dimensional test model at the Reynolds number 2.34×10^4.

In addition to using the disc difference, to get more complete information on the area around the wall, it requires the calculation of y+ on each meshing. In this study, to get the best results, the y+ used is less than 1 [3].

Based on Table 1, C_D values that tend to be smaller occur in Meshing C. One of the considerations in conducting numerical simulations is the time and memory used, then the meshing used for the next simulation is Meshing C. In this study the solver used is for steady and Turbulence models are k-ω SST.

3 Result and Discussion

3.1 Drag Coefficient Analysis

In Fig. 3, it is shown that the addition of winglets will increase drag compared to the plain wing. In this study, it can be seen that the height of the fence h = 0.5c results in a higher drag compared to the fence h = c. This applies when compared to the forward wingtip fence cant angle 90° [2] and rearward wingtip fence cant angle 90° [6]. At fence h = 0.5c also produces a higher drag than Turanoguz's research results [9]. From Fig. 3 it is found that the aspect that influences the height of the drag from the fence h = 0.5c is not just the pressure and viscous drag produced, but it must be seen other aspects that are a result of the geometry used. Other aspects include vorticity, which is one of the effects of induced drag.

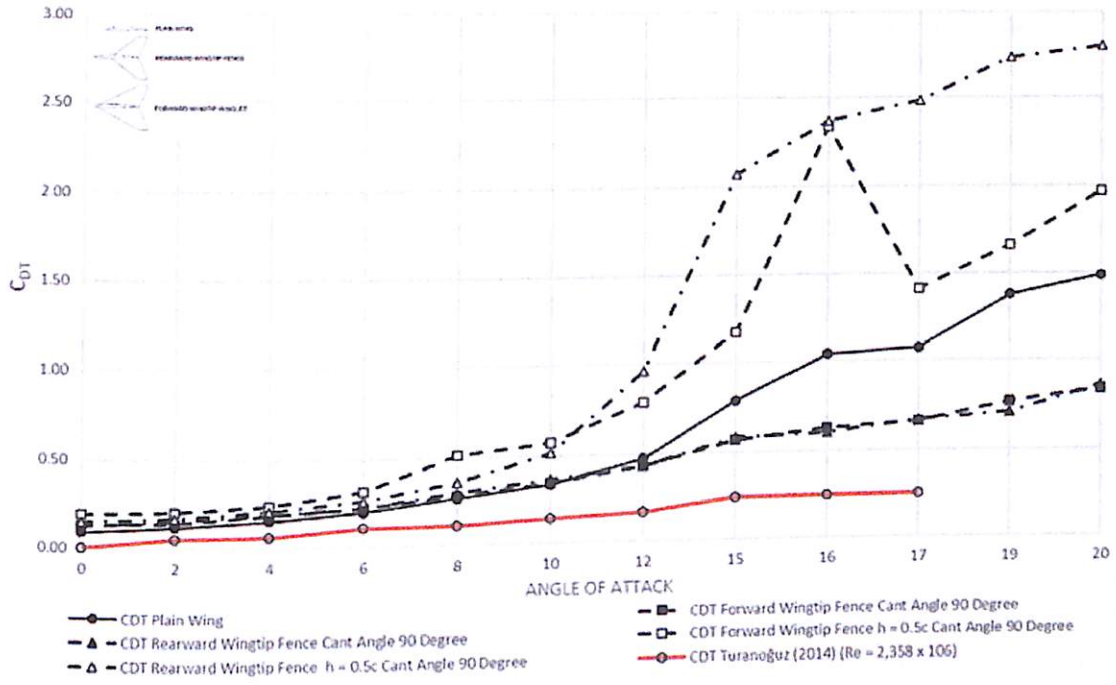

Fig. 3 C_D comparison of research results

3.2 *Lift Coefficient Analysis*

Figure 4 shows the C_L results of the study. Figure 4 also shows that the lift coefficient increases with increasing angle of attack. In the plain wing, the results of the study

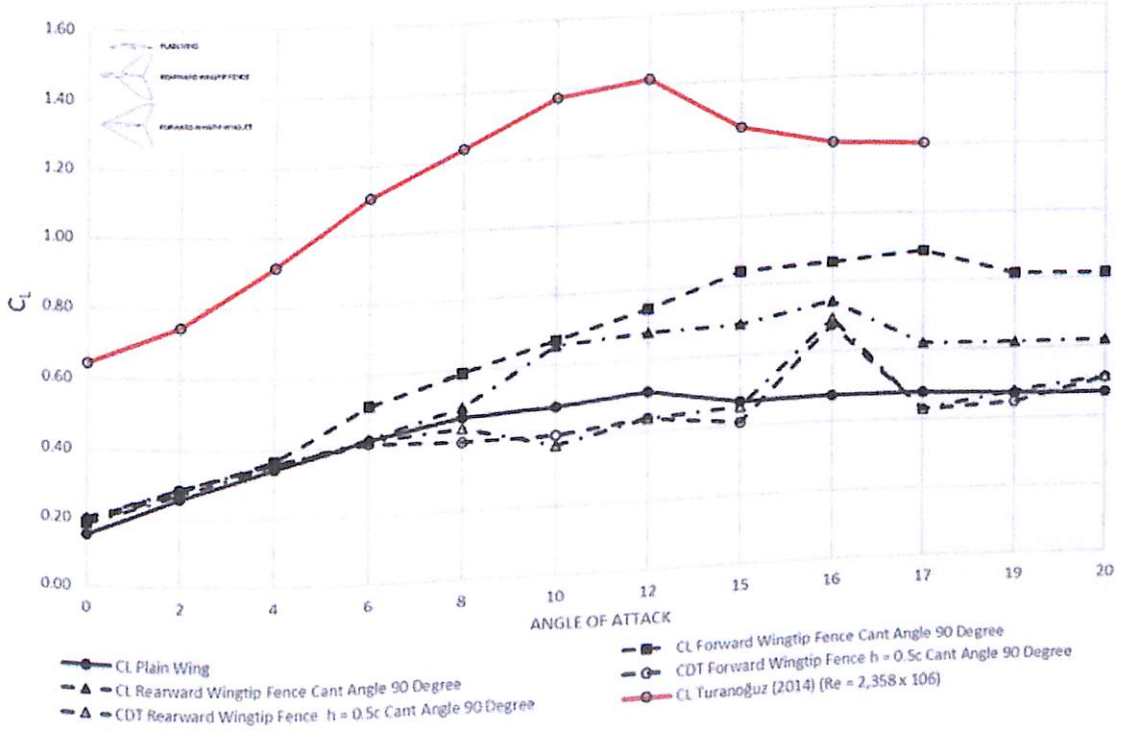

Fig. 4 C_L comparison of research results

show that stall occurs at $\alpha = 12°$. This is the same pattern as the results of Turanoguz's research [9]. In this research, fluids flow at $Re = 2.34 \times 10^4$ and Turanoguz's research at 2.34×10^6. The same pattern of the lift coefficient shows that the result quite relevant. On the forward wingtip fence cant angle 90° with fence h = c stall occurs at $\alpha = 17°$ while rearward wingtip fence cant angle 90° with fence h = c stall occurs at $\alpha = 16°$. On the forward wingtip fence cant angle 90° with fence h = 0.5c stall occurs at $\alpha = 16°$ while the rearward wingtip fence cant angle 90° with fence h = 0.5c stall occurs at $\alpha = 16°$. The results of this study indicate that the use of a wingtip fence both h = 0.5c and h = c can delay stalling.

3.3 *Lift to Drag Ratio Analysis*

Figure 5 shows the lift to drag ratio comparison of the results of the study. From Fig. 5, it can be shown that the increase in wing performance after being equipped with a forward wingtip fence cant angle 90° h = c and rearward wingtip fence cant angle 90° h = c. However, this did not occur in the forward wingtip fence cant angle 90° h = 0.5c and the rearward wingtip fence cant angle 90° h = 0.5c when compared to the plain wing. On the forward wingtip fence cant angle 90° results in higher performance than plain wing at $\alpha = 6°$ while the rearward wingtip fence cant angle

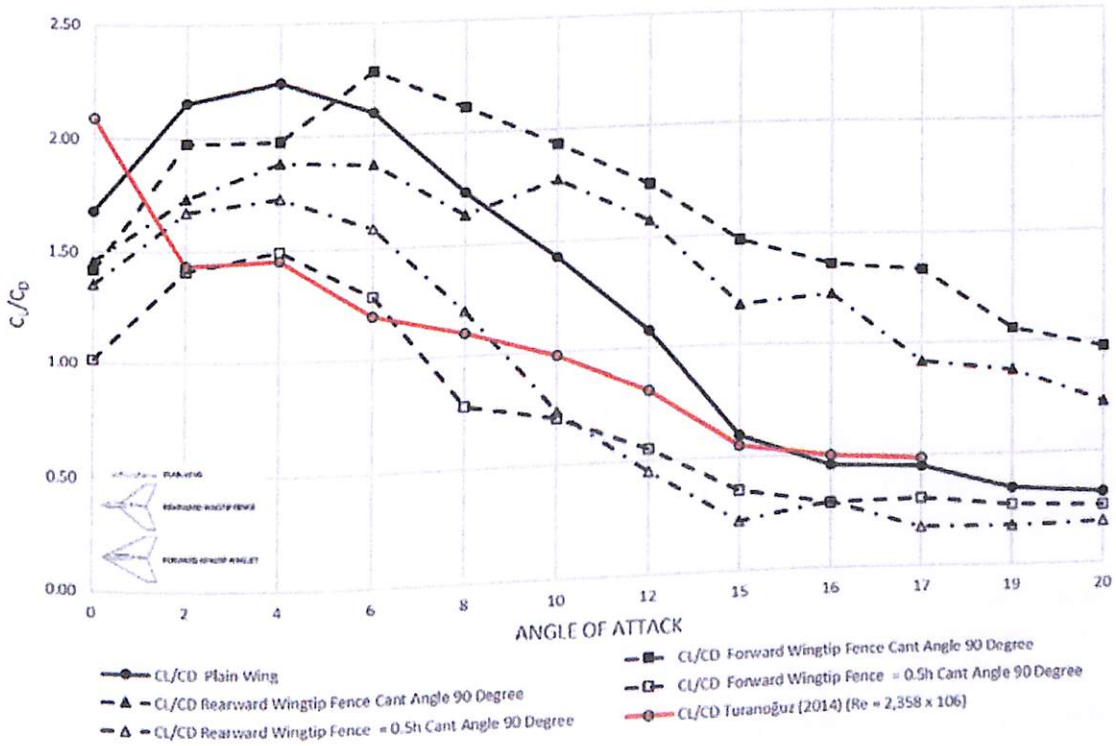

Fig. 5 C_L/C_D comparison of research results

90° produces a better performance at $\alpha = 10°$. The use of forward wingtip fence cant angle 90° h = 0.5c, and rearward wingtip fence cant angle 90° h = 0.5c have decreased aerodynamic performance at all angles of attack compared to the plain wing.

3.4 *Vorticity Magnitude Analysis*

The tendency of flow to leak around the wingtips has an important effect on the aerodynamics of the wings. This flow forms a rotating motion that leads to downstream in the trailing vortex. This vortex tip induces a small component of the velocity of air around the wing downward. This bottom component is called downwash.

The higher the angle of attack the wider the vortex formed. Vortex formation starts from the end of the trailing edge [1]. This results in a much greater vortex if the vortex has reached the leading edge. Therefore, the function of the winglet is to reduce the size of the vortex will be more perfect if the formation of the vortex is blocked from the trailing edge.

The width and concentration of the vortex is one indication of the great fluid jump from the lower surface to the upper surface of the wing. Figure 6 shows the evolution and comparison of the area of vorticity magnitude of plain wing, forward wingtip fence cant angle 90° h = c, rearward wingtip fence cant angle 90° h = c, forward wingtip fence cant angle 90° h = 0.5c, and rearward wingtip fence cant angle 90° h = 0.5c at a distance of 1 C behind the trailing edge (x = 2c). At the $\alpha = 0°$, the effect of the presence of winglets is less visible, because the vortex tip phenomenon is not very well-formed, so the results of the visualization cannot be so distinguished. Different at $\alpha = 12°$ and $\alpha = 17°$, phenomena from vortex tip can be seen more so that the difference in the form of vortex tip on the plain wing and airfoil with winglet fence can be distinguished.

From $\alpha = 12°$ and $\alpha = 17°$, it can be seen that the tip vortex on the plain wing is more concentrated in the center of the vortex. On Eppler 562 airfoil with forward wingtip fence cant angle 90° h = c, and rearward wingtip fence cant angle 90° h = c, the vortex tip that occurs is split into 2 parts.

On Eppler 562 airfoil with forward wingtip fence cant angle 90° h = 0.5c, and rearward wingtip fence cant angle 90° h = 0.5c, tend to have the shape of a plain wing but have greater value and area. It is possible that the forward and the rearward wingtip fence cant angle 90° h = 0.5c have a greater drag value.

From this visualization phenomenon it can be concluded that the use of forward wingtip fence cant angle 90° h = c and rearward wingtip fence cant angle 90° h = c is more effective to be used than the forward wingtip fence cant angle 90° h = 0.5c and the rearward wingtip fence cant angle 90° h = 0.5c because the characteristic area of vorticity is smaller than plain wing.

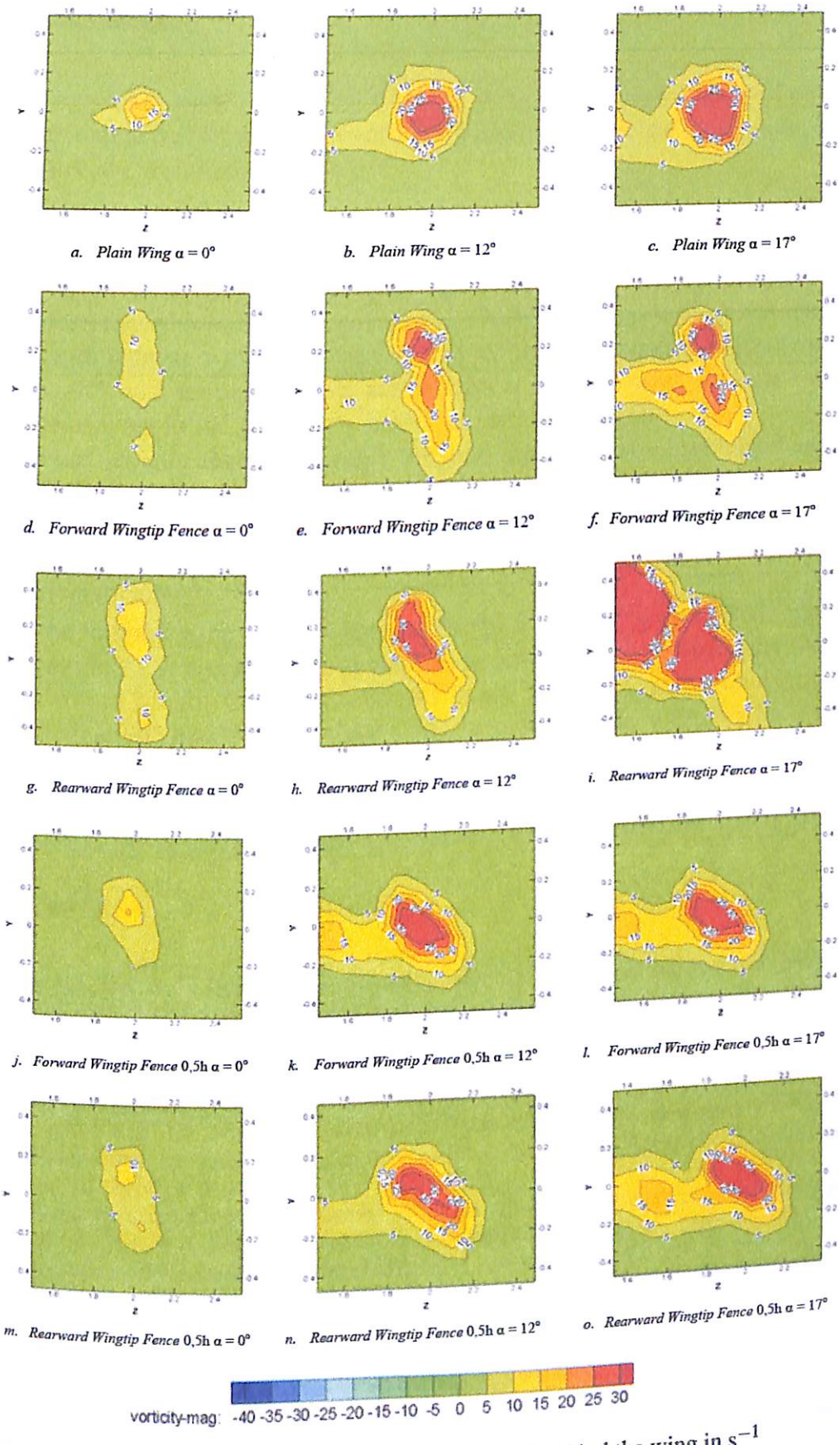

Fig. 6 Comparison of magnitude vorticity area as far as 1 C behind the wing in s^{-1}

4 Conclusion

This research has shown the effect of using winglet shape variations significantly on aerodynamic performance and vorticity. From the numerical simulation, several conclusions were shown, including:

1. Wingtip fence h = 0.5c produces higher drag compared to wingtip fence h = c. This is very much influenced by the induce drag formed by the endplate geometry.
2. The use of wingtip fence delays stalling. On the forward wingtip fence cant angle 90° with fence h = c, a stall occurs at $\alpha = 17°$. Rearward wingtip fence cant angle 90° with fence h = c, stall occurs at $\alpha = 16°$. In the forward wingtip fence cant angle 90° with fence h = 0.5c, stall occurs at $\alpha = 16°$ while rearward wingtip fence cant angle 90° with fence h = 0.5c, stall occurs at $\alpha = 16°$.
3. Forward wingtip fence cant angle 90° h = c and rearward wingtip fence cant angle 90° h = c produce an increase in aerodynamic performance. Whereas the forward wingtip fence cant angle 90° h = 0.5c and the rearward wingtip fence cant angle 90° h = 0.5c result in a decrease in the lift to drag ratio when compared to the plain wing.
4. On the forward wingtip fence cant angle 90° h = c and rearward wingtip fence cant angle 90° h = c, resulting in vortices which are divided into 2 parts. Whereas the forward wingtip fence cant angle 90° h = 0.5c and the rearward wingtip fence cant angle 90° h = 0.5c, produce vortices such as plain wing but have greater value and area.

References

1. Genç MS, Özkan G, Açikel HH et al (2016) Effect of tip vortices on flow over NACA4412 aerofoil with different aspect ratios. EPJ Web Conf 114:2–5. https://doi.org/10.1051/epjconf/201611402027
2. Hariyadi SSP, Sutardi, Widodo WA (2018) Drag reduction analysis of wing airfoil E562 with forward wingtip fence at cant angle variations of 75° and 90°. In: AIP conference proceedings
3. Kontogiannis SG, Mazarakos DE, Kostopoulos V (2016) ATLAS IV wing aerodynamic design: from conceptual approach to detailed optimization. Aerosp Sci Technol 56:135–147. https://doi.org/10.1016/j.ast.2016.07.002
4. Mulvany N, Chen L, Tu J, Anderson B (2004) Steady-state evaluation of two-equation RANS (Reynolds-Averaged Navier-Stokes) turbulence models for high-reynolds number hydrodynamic flow simulations. Dep Defence, Aust Gov 1–54
5. Myilsamy D, Thirumalai, Yokesh PP (2015) Performance investigation of an aircraft wing at various cant angles of winglets using CFD simulation. Altair Technol Conf 23
6. Setyo Hariyadi SP, Sutardi, Widodo WA (2018a) Numerical study of flow characteristics around wing airfoil Eppler 562 with variations of rearward wingtip fence. In: AIP Conference Proceedings 1983. 10.1063/1.5046207
7. Setyo Hariyadi SP, Sutardi, Widodo WA, Mustaghfirin MA (2018b) Aerodynamics analysis of the wingtip fence effect on UAV wing. Int Rev Mech Eng 12:837–846. https://doi.org/10.15866/ireme.v12ihttps://doi.org/10.15517

8. Sohn MH, Chang JW (2012) Visualization and PIV study of wing-tip vortices for three different tip configurations. Aerosp Sci Technol 16:40–46. https://doi.org/10.1016/j.ast.2011.02.005
9. Turanoguz E, Alemdaroglu N (2015) Design of a medium range tactical UAV and improvement of its performance by using winglets. In: International Conference on Unmanned Aircraft Systems, ICUAS 2015, pp 1074–1083. https://doi.org/10.1109/icuas.2015.7152399
10. Yen SC, Fei YF (2011) Winglet dihedral effect on flow behavior and aerodynamic performance of NACA0012 wings. J Fluids Eng Trans ASME 133. 10.1115/1.4004420